

Electronic band structure of titanium dioxide

N. Daude, C. Gout, and C. Jouanin

Centre d'Etudes d'Electronique des Solides, associé au Centre National de la Recherche Scientifique, Université des Sciences et Techniques du Languedoc, Place E. Bataillon, 34060 Montpellier, France

(Received 14 September 1976)

The electronic band structure of titanium dioxide is calculated by a combined tight-binding and pseudopotential method in order to interpret the numerous experimental data. The gap anisotropy is clearly shown and the values of parallel and perpendicular gaps are in good agreement with the measured ones.

I. INTRODUCTION

A great number of experimental results are available for TiO_2 . From conductivity, photoconductivity, and optical absorption, Cronmeyer¹ suggests a forbidden energy gap at 3.05 eV. Moch *et al.*² show a dichroic behavior of the absorption coefficient; the dichroism is estimated to be 11.5 meV and, moreover, the energy gap is evaluated at about 3 eV. Cardona and Harbeke³ have evaluated ϵ_2 , the imaginary part of the dielectric constant, from reflectivity between 4 and 7.87 eV. Arntz and Yacoby⁴ have performed electroabsorption measurements with polarized light; they suggest that some of the singularities are due to forbidden transitions, Frova *et al.*⁵ have obtained electroreflectance spectra with singularities in good agreement with those obtained by Cardona. Finally, Vos and Krusemeyer⁶ report an electroreflectance spectra at low nitrogen temperature; their results are in good agreement with those of Ref. 4, but they give another explanation, for them the peaks result from indirect-allowed transitions. The luminescence of TiO_2 has been studied⁷ as well and its surface properties have been investigated.⁸

We felt, in order to give a coherent interpretation of the various experimental results, that it was interesting to calculate the electronic structure of TiO_2 . In this paper we present the first calculation of the band structure of that crystal.

The unit cell is tetragonal⁹ and contains six ions. The Brillouin zone is also simple tetragonal (Fig. 1). TiO_2 is known to be strongly ionic; therefore, the valence band is mainly composed of the outermost p electrons of oxygen and the corresponding wave functions are considerably localized on O^{2-} sites. The lowest conduction band would be chiefly composed of the excited state of titanium. There are, in fact, two well-separated regions in the band structure and the two types of levels will be calculated separately by a method adapted to each situation.

The tight-binding method has been used for the valence bands. In Ref. 10 we have shown that the Robinson-Bassani-Knox-Schrieffer (RBKS) exchange potential¹¹ is well suited for the crystals with a large dielectric constant. Because of the very large dielectric constant of TiO_2 (174 along the c axis and 86 perpendicular to the c axis), we have chosen this model for the exchange potential. Details of calculations are presented in Sec. II.

For the calculation of the conduction states arising from O^{2-} ions we have used the analytic pseudopotential approach proposed by Bassani and Giuliano.¹² As we have shown elsewhere¹³ this model contains all the essential features of the actual potential, but it overestimates the repulsive effects of the p core states and for that reason the d conduction states have over high-energy values; this is why we have used a Phillips-Kleinman¹⁴ model to calculate the conduction states arising from the Ti^{4+} ions whose cores are not distorted by the crystal potential. These calculations are described in Sec. III.

II. VALENCE BANDS

We shall stress only the approximations used in giving a brief outline of the tight-binding approach. The wave functions are Bloch sums built with atomic orbitals

$$\phi_{\mu\kappa}^k(\vec{r}) = \frac{1}{\sqrt{N}} \sum_n e^{i\vec{k}\cdot(\vec{r}_\kappa + \vec{R}_n)} u_\mu(\vec{r} - \vec{r}_\kappa - \vec{R}_n). \quad (1)$$

The sum is carried over the lattice vectors \vec{R}_n . The atomic orbitals $u_\mu(\vec{r} - \vec{r}_\kappa - \vec{R}_n)$ with quantum numbers μ are centered around an atom located at $\vec{r}_\kappa + \vec{R}_n$ and \vec{r}_κ specifies the position of the κ th ion in the unit cell.

The energies are obtained by solving the secular equation

$$\det |\langle \phi_{\mu\kappa}^k | H - E | \phi_{\mu\kappa}^k \rangle| = 0. \quad (2)$$

The matrix elements of the energy operator E are two center integrals and their evaluation does not present any difficulty. The matrix elements

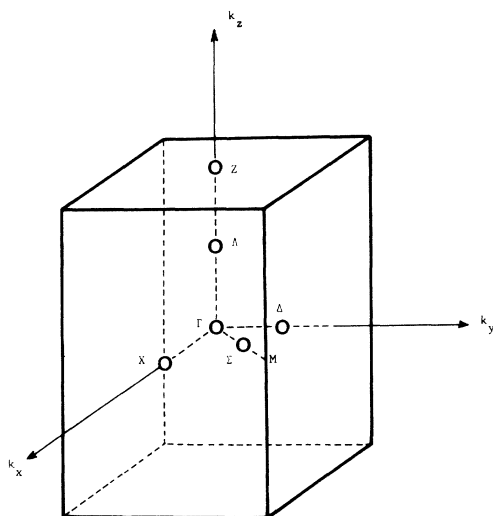


FIG. 1. Brillouin zone of simple tetragonal lattice.

of the Hamiltonian operator are more difficult to calculate. The potential produces three center terms (which are very tedious to evaluate), because it is a sum of ionic potentials. These matrix elements have been evaluated along the lines widely described in Ref. 13 and we shall not relate it again here.

We have calculated all the potential integrals larger than 0.001 Ry; for instance, in the evaluation of matrix elements between the 2s and 2p orbitals of O²⁻ ions we have carried the sum over the O²⁻ sites lying inside a sphere of a radius equal to 14 a.u.; so we have taken into account 24 or 28 neighbors according to κ and κ' values. We have used wave functions given by Clementi¹⁵ for Ti⁴⁺ ions and those calculated by Watson¹⁶ for the O²⁻ ions, and as we have shown above an RBKS exchange potential¹¹ has been chosen.

The secular equation (2) has been solved for points and axes of high symmetry of the Brillouin zone (BZ). The results for high-symmetry points are given in Table I and the energy bands are plotted in Fig. 2. The notations used to label the irreducible representations are those of Albert *et al.*¹⁷

All the states at the edges of the BZ are twofold degenerate because of the crystal symmetry (X and Z points) or because of time reversal (M point).

The first group of bands, between -1.15 and -2.269 Ry is mainly formed by the 2p states of O²⁻ ions. The maximum is the state Γ_3 at the center of the BZ; its wave function is a mixing of p_x and p_y orbitals and we should note that the transition from that state towards Γ_1 , the minimum of the conduction band, are forbidden. The next state

is Γ_5 and the transitions towards Γ_1 are also forbidden. The relative positions of the two next states Γ'_5 and Γ'_2 are important because those levels are the initial states of allowed transitions with polarized light.

The authors of Ref. 5 have shown a perpendicular light transition ($\vec{E} \perp \vec{c}$) at the edge of the BZ with an energy smaller than the parallel one ($\vec{E} \parallel \vec{c}$) which is important for the relative positions of the two levels, X_1 and X_2 .

The width of the O²⁻ 2p bands is found to be large, about 16 eV. This is surprising but we must note that with the same wave functions¹⁶ and the same potential (RBKS) we obtain, for MgO,¹⁰ an O²⁻ 2p band width of 8.52 eV in good agreement with the experiment. We think that the broad bands in TiO₂ are due to the closeness of O²⁻ ions which are nearer to one another than in MgO and to the many bonding and antibonding orbital combinations allowed by the low crystal symmetry and the large difference between them.

The second set of bands due to the 2s orbitals of O²⁻ ions is 4.25 eV wide, then the 3p bands of Ti⁴⁺ ions lie between -4.74 and -4.78 Ry.

The valence-band structure of TiO₂ is rather similar to that of MgF₂,¹³ of GeO₂,¹⁸ and of SnO₂.¹⁹

III. CONDUCTION BANDS

We have calculated the conduction states as those of an extra electron added to the lattice and under the potential of the filled ionic shells. We have used the analytical pseudopotential proposed by Bassani *et al.*¹² for the conduction states of the O²⁻ ions and the pseudopotential model of Phillips and

TABLE I. Energy levels (in Ry) of the valence states of TiO₂. The notations are those of Ref. 17.

Γ_1	-1.321	-3.176			
Γ_2	-2.369				
Γ_3	-1.152				
Γ_4	-2.254	-2.863			
Γ_5	-1.254				
Γ'_2	-1.283	-4.747			
Γ'_3	-1.489	-4.769			
Γ'_5	-1.255	-1.799	-2.937	-4.741	-4.786
Z_1	-1.683	-2.192	-3.00	-4.80	
Z_2	-1.765				
Z_3	-1.385	-2.877	-4.769		
Z_4	-1.382	-1.895	-4.764		
X_1	-1.171	-1.472	-2.055	-2.197	-3.132
X_1	-4.756	-4.776			
X_2	-1.181	-1.346	-4.759		
M_1, M_4	-2.03	-3.04			
M_2, M_3	-1.367				
M_5	-1.224				
M'_2, M'_3	-1.247	-4.759			
M'_5	-1.283	-2.228	-3.03	-4.745	-4.786

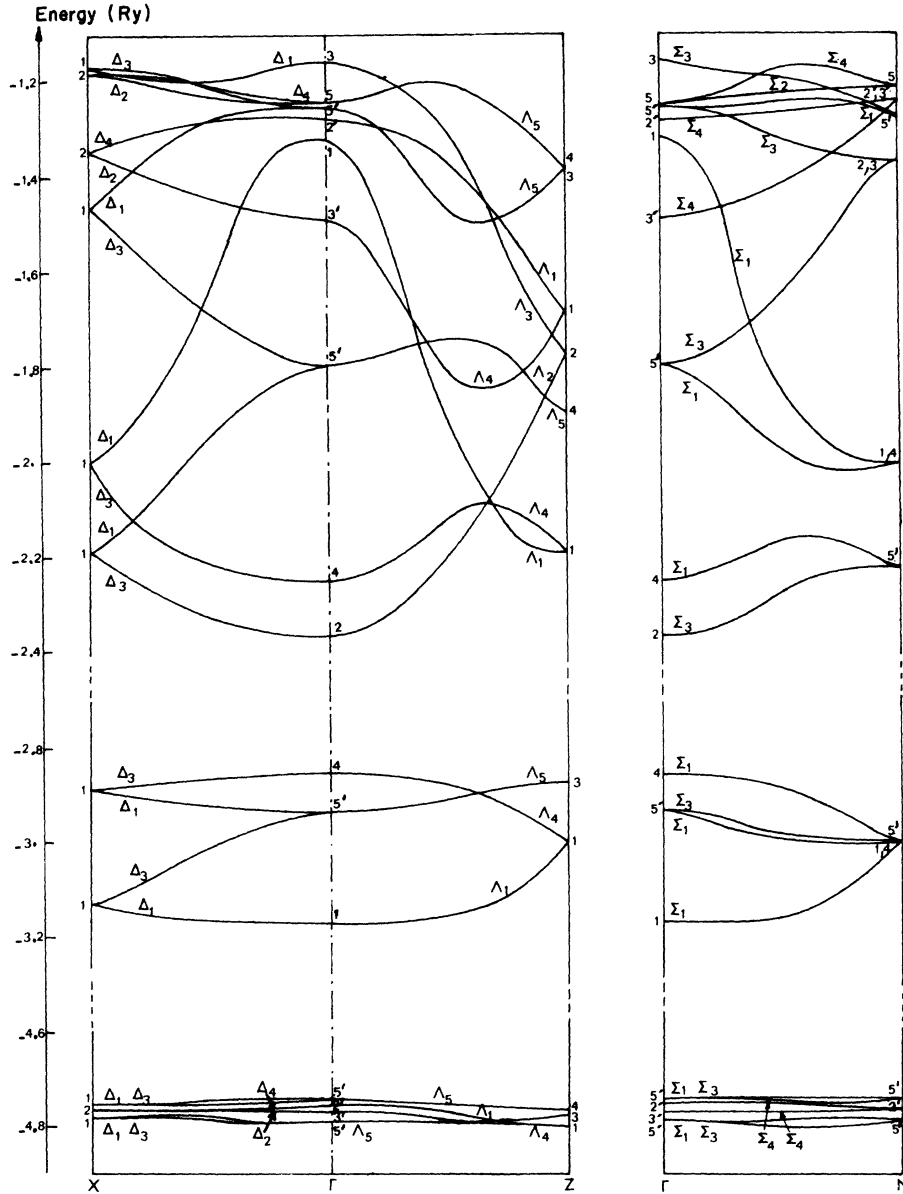


FIG. 2. Valence bands of TiO_2 . Symmetry notations are those of Ref. 17.

Kleinman¹⁴ for those of the Ti^{4+} ions. The reasons for using this method are widely exposed in Refs. 10 and 13 as are the details of the calculations and we shall not repeat them here.

We shall mention only that the two empirical parameters α_i and A_i which appear in the analytical pseudopotential are the same as those used in the calculations of the conduction states of MgO and CaO .¹⁰

Our calculations include about 200 plane waves, enough to obtain a good convergence. Because of the low crystal symmetry the matrices to be diagonalized are larger than in the cubic system and at the M point they are complex. The results

we obtain are reported in Fig. 3 and Table II.

The lower conduction band is broad with a minimum at Γ_1 . As the maximum of the valence states in Γ_3 and the $\Gamma_3 \rightarrow \Gamma_1$ transition is unallowed by the transition rules at the first order, the first allowed direct transition will be $X_1 \rightarrow X_1$. So, our energy-band scheme shows many possibilities of indirect allowed transitions such as $X_1 \rightarrow \Gamma_1$ and $X_2 \rightarrow \Gamma_1$.

IV. COMPARISON WITH EXPERIMENTAL RESULTS

The experimental works of the Refs. 1-6 are in fairly good agreement with each other, but the optical constant behavior is only known up to 8 eV.

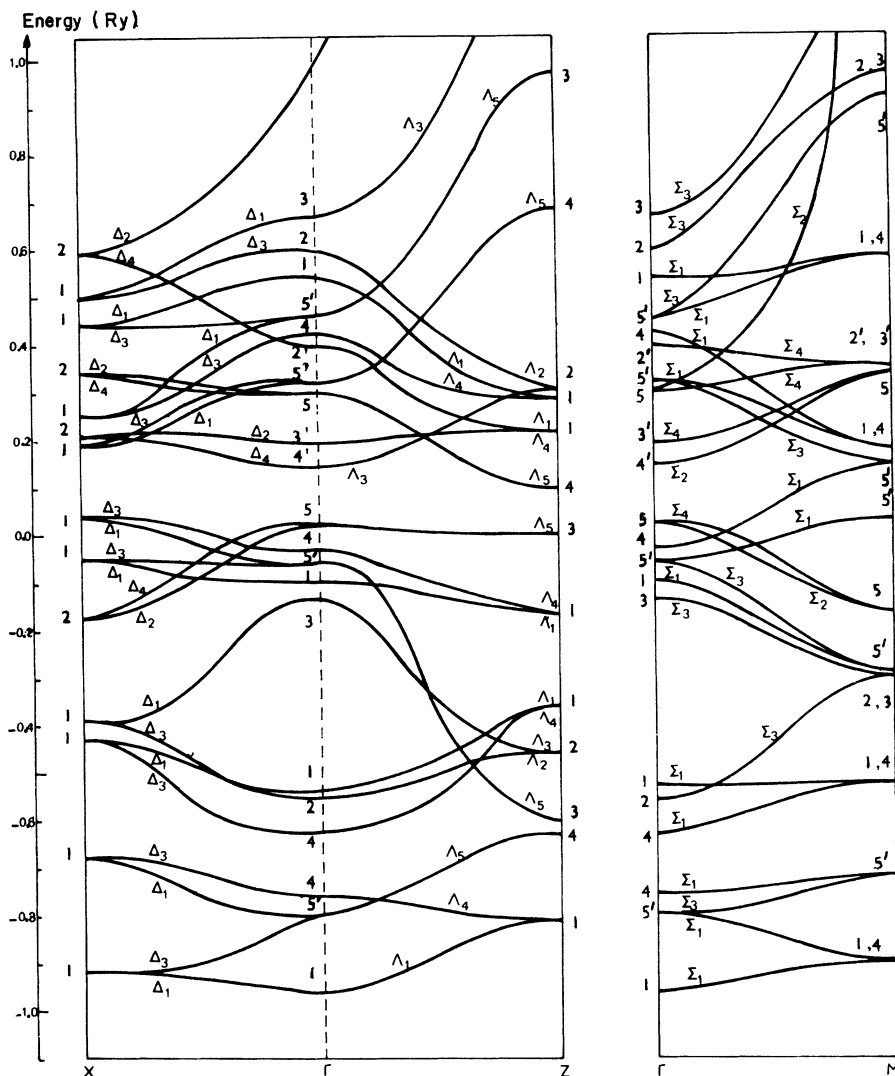


FIG. 3. Conduction bands of TiO_2 . Symmetry notations are those of Ref. 17.

By measuring conductivity, photoconductivity, and optical absorption with natural light, Crone-meyer¹ deduces a forbidden energy gap of 3.05 eV with a singularity at about 3.3 eV.

Moch *et al.*² deduce from their absorption coefficient measurement the dichroic behavior of the rutile; the dichroism is 11.5 meV. Moreover they place the 4s band of Ti^{4+} 3.3 eV above the valence band.

The energies of the peaks of the imaginary part of the dielectric constant obtained by Cardona and Harbeke³ are: 4.0, 5.35, 6.1, 7.04, and 8.05 with $\vec{E} \perp \vec{c}$ and: 4.11, 6.63, and 7.87 eV with $\vec{E} \parallel \vec{c}$.

The values of the singularities of the electroreflectance spectra measured by Frova *et al.*⁵ are in good agreement with those of Cardona, but their curves show two singularities which did not appear in the preceding data; the first one at 3.3 eV with

$\vec{E} \perp \vec{c}$ and the other at 3.4 eV with $\vec{E} \parallel \vec{c}$.

Arntz and Yacobi,⁴ by electroadsorption, measure peaks at 3.026 eV with $\vec{E} \perp \vec{c}$ and 3.029 eV with $\vec{E} \parallel \vec{c}$; they attribute them to indirect transitions. A structure which appears near 3.11 eV is attributed to an unallowed direct transition.

Vos and Krusemeyer⁶ report an electroreflectance spectrum at liquid-nitrogen temperature. They obtain structures at 3.026 eV with $\vec{E} \perp \vec{c}$ and at 3.059 eV with $\vec{E} \parallel \vec{c}$, that we can compare with the preceding values of Arntz and Yacoby. A structure centered around 3.13 eV which appears with both $\vec{E} \perp \vec{c}$ and $\vec{E} \parallel \vec{c}$ is identified with the structure near 3.11 eV of Ref. 4 and is explained by an indirect-allowed transition.

In order to simplify the discussion, we have sketched on Fig. 4 all the direct- and indirect-allowed transitions with an energy lower than 11

TABLE II. Energy levels (in Ry) of the conduction states of TiO₂. The notations are those of Ref. 17.

Γ_1	-0.9567	-0.532	-0.1016	0.539	0.777	
Γ_2	-0.5646	0.660				
Γ_3	-0.143	0.626				
Γ_4	-0.7567	-0.6308	-0.035	0.411	1.514	
Γ_5	0.0217	0.275	1.326			
Γ'_1	1.19					
Γ'_2	0.396	1.283				
Γ'_3	0.192	1.131				
Γ'_4	0.146					
Γ'_5	-0.798	-0.06	0.293	0.462	0.990	1.019
Z_1	-0.812	-0.364	-0.167	0.217	0.286	
Z_2	-0.458	0.322	1.116			
Z_3	-0.595	0.0017	0.969			
Z_4	-0.634	0.103	0.687	1.255		
X_1	-0.917	-0.680	-0.429	-0.3947	-0.0485	0.0375
X_1	0.1946	0.254	0.4426	0.705	0.859	
X_2	-0.169	0.210	0.340	0.593	1.189	
M_1, M_4	-0.903	-0.5296	0.1839	0.578	1.429	
M_2, M_3	-0.296	0.9667	1.58			
M_5	-0.164	0.339	0.960	1.542		
M'_2, M'_3	0.342	0.997				
M'_5	-0.72	-0.283	+0.0295	0.157	0.925	1.095

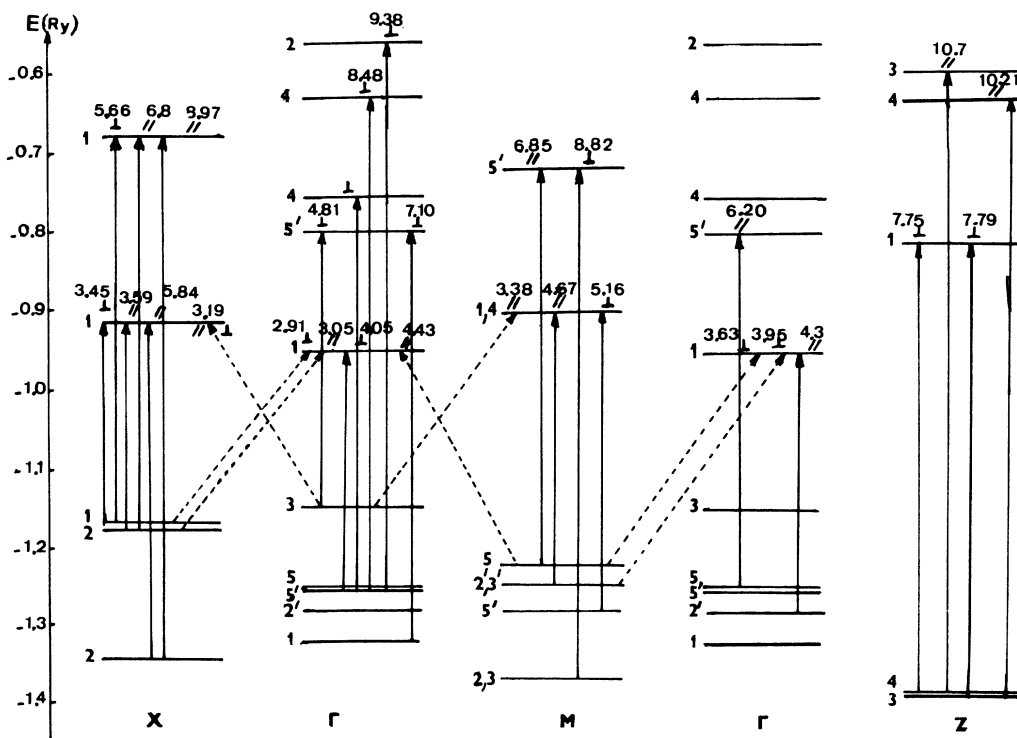


FIG. 4. Sketch of the direct- and indirect-allowed transitions with polarized light.

TABLE III. Comparison between experimental and theoretical values.

	Ref. 3	Ref. 5	Ref. 4	Ref. 6	Theory	Identification
$\vec{E} \perp \vec{c}$			3.026	3.026	2.91	$X_1 \rightarrow \Gamma_1$
			3.114	3.13	3.19	$\Gamma_3 \rightarrow X_1$
		3.3			3.45	$X_1 \rightarrow X_1$
	4.0	4.07			4.05	$\Gamma_5 \rightarrow \Gamma_1$
	5.35	5.35			4.81	$\Gamma_3 \rightarrow \Gamma_5$
	6.1				6.66	$X_1 \rightarrow X_1$
	7.4				6.7	$\Gamma_5 \rightarrow \Gamma_4$
	8.05				7.54	$X_1 \rightarrow X_1$
$\vec{E} \parallel \vec{c}$			3.029	3.059	3.05	$X_2 \rightarrow \Gamma_1$
			3.114	3.13	3.19	$\Gamma_3 \rightarrow X_1$
		3.4			3.59	$X_2 \rightarrow X_1$
	4.11	4.15			4.3	$\Gamma_2 \rightarrow \Gamma_1$
	6.63				6.8	$X_2 \rightarrow X_1$
					6.85	$M_5 \rightarrow M'_5$
					8.9	$X_2 \rightarrow X_1$

eV, both with $\vec{E} \perp \vec{c}$ and $\vec{E} \parallel \vec{c}$.

We can see that the lowest transitions are indirect ones, namely, $X_1 \rightarrow \Gamma_1$ (2.91 eV with $\vec{E} \perp \vec{c}$) and $X_2 \rightarrow \Gamma_1$ (3.05 eV with $\vec{E} \parallel \vec{c}$). These two values can be compared with the experimental ones of 3.026 eV with $\vec{E} \perp \vec{c}$ and 3.029 and 3.059 eV with $\vec{E} \parallel \vec{c}$, of Refs. 4 and 6.

We evaluate the indirect transition $\Gamma_3 \rightarrow X_1$ at 3.19 eV; this transition is allowed with both $\vec{E} \perp \vec{c}$ and $\vec{E} \parallel \vec{c}$ and can explain the structure observed by the authors of Refs. 4 and 6, respectively, around 3.11 and 3.13 eV.

The first direct-allowed transitions are at the X edge of the BZ; $X_1 \rightarrow X_1$ (3.45 eV with $\vec{E} \perp \vec{c}$) and $X_2 \rightarrow X_1$ (3.59 eV with $\vec{E} \parallel \vec{c}$). This result agrees both qualitatively and quantitatively with the experimental observation of Frova *et al.*⁵ (transitions at 3.3 and 3.4 eV with $\vec{E} \perp \vec{c}$ and $\vec{E} \parallel \vec{c}$, respectively).

In Table III we propose an interpretation of the other experimental singularities. As we can see the agreement between experimental and theoret-

cal results is good. We ought to note that the experimental values of the dichroism (11.5 meV,² 33 meV,⁶ and³ 110 meV) are smaller than ours (140 meV); however, we think that, with such weak energies, both experimental errors and theoretical approximations are responsible for this fact.

V. CONCLUSION

In this paper the energy bands of TiO₂ have been obtained for the first time in order to interpret the numerous experimental data. We have performed this calculation by two complementary methods taking into account the characteristics of each electron type. In particular, it is shown that the tight-binding scheme gives good results with an RBKS exchange potential for materials with a large dielectric constant. It is also shown that the O²⁻ pseudopotential parameters previously obtained by adjusting the gaps of MgO and CaO give good results for the conduction states of TiO₂.

¹D. C. Cronemeyer, Phys. Rev. **87**, 876 (1952).

²P. Moch, M. Balkanski, and P. Aigrain, C. R. Acad. Sci. (Paris) **251**, 1373 (1960).

³M. Cardona and G. Harbeke, Phys. Rev. **137**, 1467 (1965).

⁴F. Arntz and Y. Yacoby, Phys. Rev. Lett. **17**, 857 (1966).

⁵A. Frova, P. J. Body, and Y. S. Chen, Phys. Rev. **157**, 157 (1967).

⁶K. Vos and H. J. Krusemeyer, Solid State Commun. **15**, 949 (1975).

⁷R. R. Addis, A. K. Ghosh, and F. G. Wakin, App. Phys. Lett. **12**, 397 (1968).

Let. **12**, 397 (1968).

⁸V. E. Henrich, G. Dresselhaus, and H. S. Zeiger, Solid State Research Report, Lincoln Laboratory, M.I.T., 1975 (unpublished).

⁹R. W. G. Wyckoff, *Crystal Structure* (Interscience, New York, 1957).

¹⁰N. Daude, C. Jouanin, and C. Gout, Phys. Rev. B (to be published).

¹¹J. E. Robinson, F. Bassani, R. S. Knox, and J. R. Schrieffer, Phys. Rev. Lett. **9**, 215 (1962).

¹²F. Bassani and E. S. Giuliano, Nuovo Cimento B **8**, 193 (1972).

- ¹³C. Jouanin, thesis (Montpellier, 1974) (unpublished); C. Jouanin, J. P. Albert, and C. Gout, *Nuovo Cimento B* 28, 483 (1975); C. Jouanin, J. P. Albert, and C. Gout, *J. Phys. (Paris)* 37, 595 (1976).
- ¹⁴J. C. Phillips and L. Kleinman, *Phys. Rev.* 116, 287 (1959).
- ¹⁵C. Clementi, *Tables of Atomic Functions*, IBM Corporation, San José, 1965 (unpublished).
- ¹⁶R. G. Watson, *Phys. Rev.* 111, 1108 (1958).
- ¹⁷J. P. Albert, C. Jouanin, and C. Gout, *Phys. Status Solidi* 47, 451 (1971).
- ¹⁸F. J. Arlinghaus and W. A. Albers, *J. Phys. Chem. Solids* 32, 1455 (1971).
- ¹⁹F. S. Arlinghaus, *J. Phys. Chem. Solids* 35, 931 (1974).